Heterogeneous photocatalytic degradation of 4-nitrophenol by visible light responsive TiO_2-polyaniline nanocomposites

K. P. Sandhya and S. Sugunan

ABSTRACT

Different compositions of TiO_2-polyaniline composites were prepared via chemical oxidative polymerisation of aniline over TiO_2 nanoparticles followed by hydrothermal treatment. The prepared composites were characterised by various physicochemical techniques. From UV-VIS digital replay system (DRS) analysis, the shifts of the absorption maximum towards the visible region are indicated and transmission electron microscopy analysis showed that the particle size of TiO_2 is reduced after incorporation of polyaniline. The photocatalytic activity of visible light responsive polyaniline modified TiO_2 in the degradation of 4-nitrophenol was studied. The percentage degradation was monitored using a UV-VIS spectrophotometer. About 92% degradation was obtained with polyaniline modified TiO_2.

Key words | 4-nitrophenol degradation, photocatalysis, TiO_2-polyaniline nanocomposites

K. P. Sandhya
S. Sugunan (corresponding author)
Department of Applied Chemistry,
Cochin University of Science and Technology,
Cochin-682022,
Kerala,
India
E-mail: *ssg@cusat.ac.in*

INTRODUCTION

The pollution of drinking water reservoirs and the aquatic environment by chemicals is a serious problem nowadays. Nitro aromatic compounds are recognized as environmentally hazardous. Nitrophenols are some of the most refractory substances present in industrial wastewaters because of their high stability and solubility in water (Paola *et al*. 2003). As a waste product, polynitrophenols (PNP) are hazardous and are a priority toxic pollutant used in pharmaceutical manufacturing, fungicides, insecticides and dyes. 4-Nitrophenol (4-NP) can be released into the soil as a result of hydrolysis of several organophosphates, including pesticides such as parathion and methyl parathion. Animal studies suggest that PNP may cause blood disorders. It is difficult to purify PNP-contaminated wastewater as a result of it being stable towards chemical and biological degradation (Yang *et al*. 2010). There is convincing evidence that 4-NP is one of the secondary pollutants formed in the tropospheric transformation of monoaromatic chemicals with NOx and ozone. Purification of wastewater contaminated with 4-NP is very difficult indeed. The presence of a nitro substituent is known to render benzenoid compounds more resistant to microbial degradation. 4-NP is very photostable, a phenomenon believed to be due to the charge transfer character of its triplet state. In aqueous aerated solutions, 4-NP is very reluctant to undergo photochemical transformations (Kochany 1991). Nitrophenols are involved in the synthesis of many products and appear in the degradation of pesticides like parathion (Meallier *et al*. 1977) and nitrofen (Nakagawa & Crosby 1974).

From a catalytic point of view, TiO_2 possesses a unique type of surface involving both redox and acid–base sites. In addition to high thermal stability, its amphoteric character makes titania a promising catalytic material. The textural and acid–base properties of titania depend greatly on the method of preparation. Loading of sulphate using sulphuric acid makes TiO_2 more acidic as its surface is positively charged due to protonation. Krishnakumar in 2011 reported the green synthesis of N-formylation of amines at room temperature using nano-TiO_2-SO_4^{2-} (Krishnakumar & Swaminathan 2011a). They also reported an efficient protocol for the green synthesis

doi: 10.2166/aqua.2014.018

of quinoxaline and dipyridophenazine derivatives at room temperature using sulfated titania (Krishnakumar & Swaminathan 2011a, b). The photocatalytic degradation rate of the different nitrophenols depends on various parameters, such as temperature (Chen & Ray 1998), pH (Augugliaro *et al*. 1993; Chen & Ray 1998) and initial concentration of the pollutant (Nakagawa & Crosby 1974; Meallier *et al*. 1977; Augugliaro *et al*. 1991; Chen & Ray 1998). Here in this work we have tried to degrade nitrophenol using visible light responsive polyaniline-modified TiO_2 systems and achieved around 92% degradation.

EXPERIMENTAL

Preparation of catalysts

Pure TiO_2 (T)

Titanium isopropoxide and acetic acid in a volume ratio 1:2 were taken in a beaker and magnetically stirred with dropwise addition of distilled water from a dropping funnel. The clear solution obtained was mixed with the solution of the surfactant P123 in water and the mixed solution was then sonicated for 3 hours. It was then transferred to an autoclave and kept overnight at 110 °C. The resultant mixture was then filtered and dried in an air oven at 110 °C followed by calcination at 500 °C for 5 hours.

TiO_2-PANI (TP)

Ammonium peroxodisulphate solution (12.5 g in 100 ml) was added dropwise to a mixture of 2.5 g TiO_2 in 100 ml 1 M HCl solution and 5 ml of distilled aniline kept in an ice bath under constant stirring. The mixture, after sonication for about 3 hours, was transferred to an autoclave and kept overnight at 110 °C. The mixture was then filtered, washed with water and acetone to remove unreacted aniline, and dried in an oven at 110 °C. Three different compositions of the nanocomposites were made by varying the molar ratio of titanium dioxide and aniline and they were named as TP1(4:1), TP2(2:1) and TP3(1:1).

Characterization

X-ray diffraction (XRD) patterns were recorded in a Bruker AXS D8 Advance X-Ray diffractometer using Ni filtered Cu Kα radiation ($\lambda = 1.5406$ Å) in the range 5–70° at a scan rate 2°/min. The IR spectra of the samples were recorded using a Thermo NICOLET 380 Fourier transform infrared spectroscopy (FTIR) Spectrometer by means of KBr pellet procedure. UV-digital replay system (DRS) spectra were taken in a UV-VIS double beam UVD-3500, Labomed Inc. spectrophotometer. Determination of surface area of the samples was achieved in a Micromeritics Tristar 3000 surface area analyzer. Prior to the measurements, the samples were degassed at 110 °C for 6 h. TG/DTA analysis was done on a PerkinElmer Pyris Diamond thermogravimetric/differential thermal analyzer instrument under a nitrogen atmosphere at a heating rate of 5–10°/min from room temperature to 1,000 °C. Morphology of all samples was observed on a PHILIPS, CM200, operating voltages: 20–200 kv; resolution: 2.4 Å. Raman spectra were recorded on a Horiba Jobin Yvon Lab Ram HR system at a spatial resolution of 2 mm in a backscattering configuration. The 514.5 nm line of Argon ion laser was used for excitation. X-ray photoelectron spectroscopy (XPS) measurement was performed using SPECS XPS system with 150 W achromatic Al Kα X-ray source at 1,486.6 eV energy. The survey scans were obtained at 70 eV pass energy and composition was obtained from survey scan. Core level spectra of C1 s was obtained at 25 eV pass energy and Ti 2p and O1 s core levels at 40 eV pass energies. C1 s and Ti 2p core levels were deconvoluted with Gaussian-Lorenztian to get component peaks.

Photocatalytic experiment

The photocatalytic activities of the samples were evaluated by the degradation of 4-NP. Photocatalytic activities of the prepared systems were scanned using Oriel Uniform illuminator (Newport Model 66901). For a typical reaction, 10 ml of 10^{-4} M aqueous 4-NP solution was used. A high pressure ozone free xenon lamp served as the visible light source; a glass filter was added to allow visible light (>400 nm) to pass through. The light source is a 150 W Xe lamp with an irradiation intensity of 96.8 mW cm^{-2}. Before illumination,

the suspensions were stirred for 30 min in the dark in order to reach adsorption–desorption equilibrium between the photocatalyst and 4-NP solution and the irradiation was performed for about 1 hour. After irradiation the percentage degradation was monitored using a UV-VIS spectrophotometer.

RESULTS AND DISCUSSION

Wide angle XRD

The XRD pattern of TiO_2 and polyaniline modified TiO_2 are shown in Figure 1. Pure titania showed the presence of only the photocatalytically active anatase phase with $2\theta = 25.5$ (1,0,1 plane), 38 (0,0,4) plane, 48.3 (2,0,0) plane, 54 (1,0,5) plane, 55.2 (2,1,1) plane, 63 (2,0,4) plane, 68.9 (1,1,6) plane. No characteristic peaks of rutile or brookite phases were observed indicating high purity of the system. When PANI is adsorbed onto the surface of TiO_2, the molecular chain of adsorbed PANI is tethered and the degree of crystallinity decreases (Zhang *et al.* 2006).

Titania polyaniline composites exhibited the characteristic peaks of anatase phase with a slight lowering of intensity. PANI incorporation had no significant effect on the crystallization and phase characteristics of TiO_2. Increase in the amount of polyaniline resulted in a further lowering of intensity of the diffraction peaks.

Optical absorption spectra

Figure 2 shows the UV-VIS absorption spectra of pure TiO_2 and polyaniline modified TiO_2. Clearly, the resulting PANI-TiO_2 composite can strongly absorb not only the near ultraviolet light but also the visible light, whereas the TiO_2 can absorb light with wavelengths below 250 nm only (Guo *et al.* 2012).

Polyaniline incorporation extended the absorption of TiO_2 to the visible region as far as 800 nm compared with the bare TiO_2 (Liao *et al.* 2011). Above 400 nm, only the composite shows absorption and a broad peak in the range 500–750 nm, indicating the presence of the PANI on the surface of the TiO_2 nanoparticles (Salem *et al.* 2009).

N_2-adsorption–desorption studies

The N_2 adsorption/desorption isotherms and Barrett–Joyner–Halenda pore size distributions of the prepared sample is displayed in Figure 3. All the prepared samples show type IV isotherm with an H1 type hysteresis loop. Pure TiO_2 shows a surface area around 56.87 $m^2 g^{-1}$. In the case of 4:1 composite (TP1) surface area is 45.14 $m^2 g^{-1}$, 2:1 composite (TP2) it is 46.04 $m^2 g^{-1}$ and finally for 1:1 composite (TP1) it is 39.32 $m^2 g^{-1}$. Polyaniline incorporation results in a drastic decrease in pore volume and an increase in pore diameter compared with TiO_2. As we incorporate the conducting polymer in to the titania, the surface

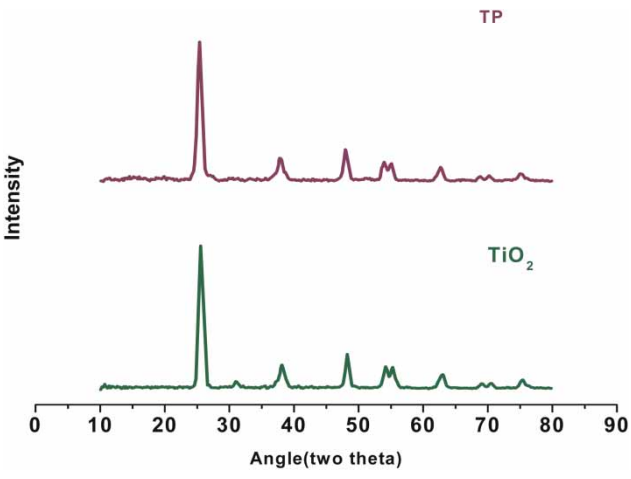

Figure 1 | XRD Pattern of pure TiO_2 and polyaniline modified TiO_2 (TP).

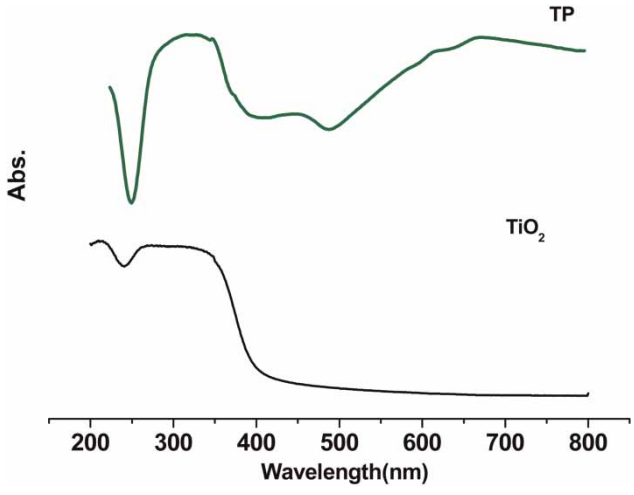

Figure 2 | UV-VIS DRS spectra of pure TiO_2 and polyaniline modified TiO_2 (TP).

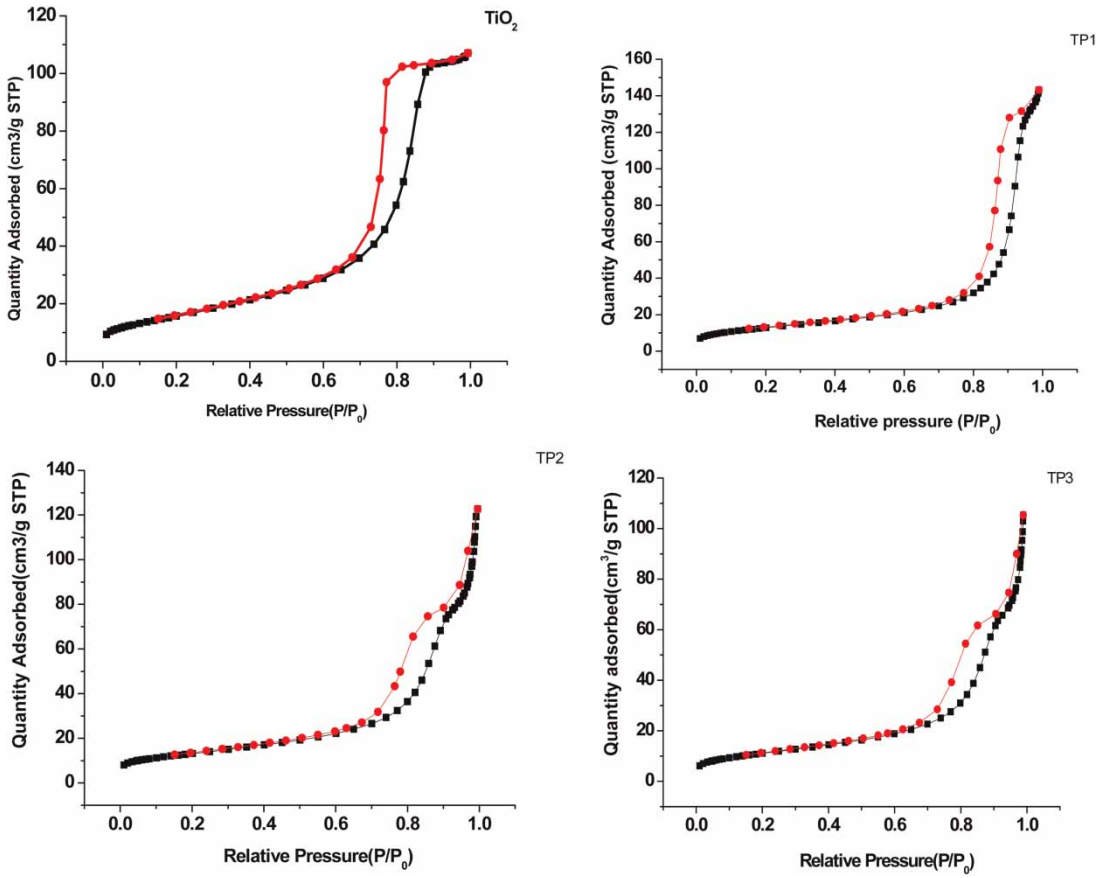

Figure 3 | N_2 adsorption–desorption isotherms and pore diameter distributions of pure and polyaniline modified TiO_2 samples.

area and pore volume decreases and the pore diameter increases. The change in pore diameter is drastic when we incorporate lower amounts of the polymer and the change is not so great as the amount of polymer in the composite increases. This may be due to the fact that at lower monomer concentration the rate of diffusion of monomer in to the pore channels of the titania is comparable to that of the rate of polymerisation. So there is a chance of polymer formation inside the pore channels. This results in a pore volume decrease and may cause the expansion of the pores which results in an increase in pore diameter. But as the concentration or amount of monomer increases the rate of polymerisation is high compared to the rate of diffusion. So the polymerisation occurs at the surface before the monomer diffuses in to the pore channels. This may cause pore blockage which results in a decrease in surface area and pore volume but the change in pore diameter is not so prominent.

FTIR spectra

IR spectra of pure TiO_2 and polyaniline, along with the composites are shown in Figure 4. Pure TiO_2 shows peaks around 456, 1,623, 3,441 cm^{-1}, which may be attributed to the Ti-O-Ti stretching, O-H bending, and O-H stretching, respectively.

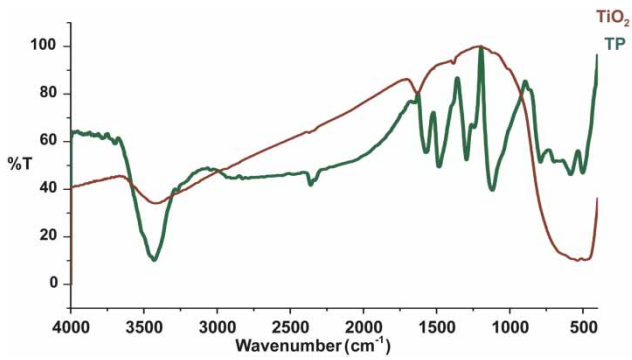

Figure 4 | FTIR spectra of pure TiO_2 and polyaniline modified TiO_2 (TP).

Peaks for pure polyaniline appears at around 503 cm^{-1} (C-H out of plane bending vibration), 808 cm^{-1} (para-substituted aromatic rings), 1,133 cm^{-1} (C-H in plane bending) and 1,294 cm^{-1} (C-N stretching). Two bands in the range 1,450–1,600 cm^{-1} (1,491, 1,581 cm^{-1}) can be assigned to the nonsymmetric C6 ring stretching modes. Higher frequency mode has a higher contribution from the quinoid ring and a lower one from the benzenoid ring. Peaks around 3,445 cm^{-1} corresponds to N-H stretching whereas aromatic C-H stretching results in a band in the range 3,000–2,500 cm^{-1} (Ganesan & Gedanken 2008).

PANI-TiO_2 composites retained almost all the peaks of PANI and TiO_2. PANI is believed to undergo polymerization on the surface of TiO_2. Peaks at 1,645 cm^{-1} (bending mode of water) and 3,448 cm^{-1} (stretching mode of water) suggest the presence of water even after calcination. This is quite important since surface hydroxyl groups provide higher capacity for oxygen adsorption which is essential for the photocatalytic activity of anatase (Ohtani *et al.* 1997).

Raman spectra

Raman spectra recorded for TiO_2 and TiO_2-PANI nanocomposites are shown in Figure 5. In the Raman spectrum of the anatase TiO_2 the following modes can be assigned: ~144 (Eg), 197 (Eg), 399 (B1g), 513 (A1g), 519 (B1g) and 639 cm^{-1} (Eg).

Raman spectra of TiO_2-polyaniline composites showed two additional peaks at 1,337 and 1,573 cm^{-1} corresponding to C-N and C = C stretching, respectively, of the polymer chain. This confirmed the incorporation of polyaniline into titania (Huyen *et al.* 2011).

Thermogravimetric analysis

The TG-derivative thermogravimetric (DTG) curves of pure TiO_2 and polyaniline/TiO_2 nanocomposites with various weight percentages are shown in Figure 6. In the case of TiO_2 the weight loss around 100 °C is due to the elimination of water and a major weight loss around 100–250 °C is due to the volatilization of water of hydration, and at around 300–400 °C is due to combustion of organic species such as P123 and CH_3COOH (Liu *et al.* 2009).

In the case of the composite, three major weight losses were observed: the first around 100 °C due to the elimination of water, the second around 260 °C corresponds to the loss of dopant HCl and the final weight loss at high temperature around 450 °C is due to the breaking of the polymer backbone (Danielle *et al.* 2003).

X-ray photoelectron spectroscopy

XPS spectra of both pure and modified TiO_2 are represented in Figure 7. In the X-ray photoelectron spectra of PANI modified TiO_2, the elements C, O, Ti and N can be detected and

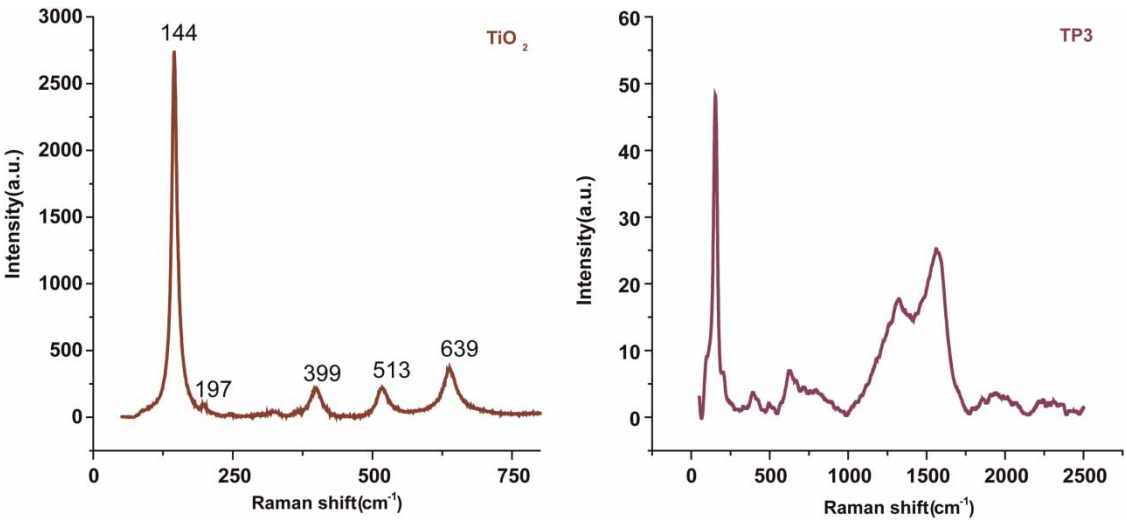

Figure 5 | Raman spectra of pure TiO_2 and polyaniline modified TiO_2 (TP).

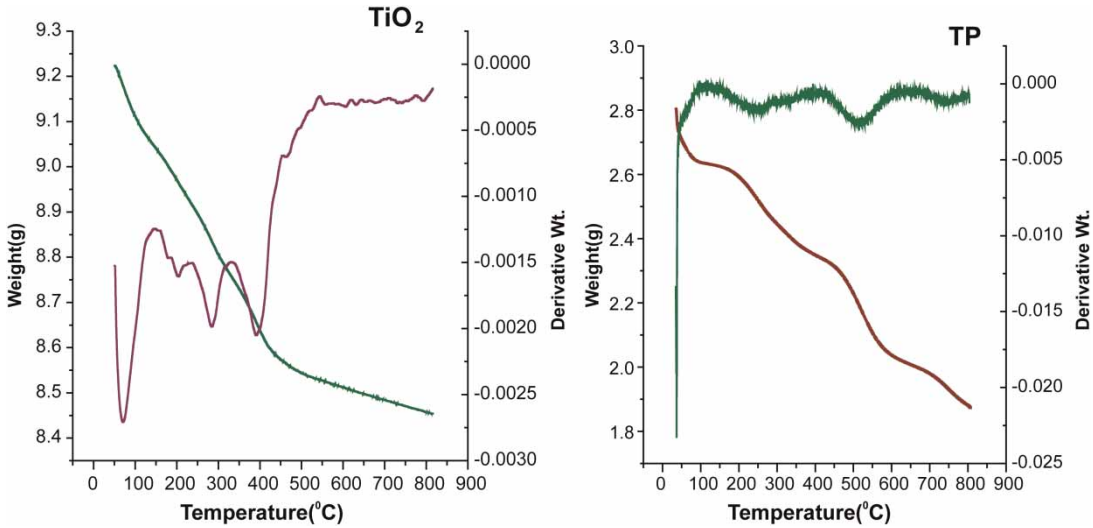

Figure 6 | TG-DTG pattern of pure TiO_2 and polyaniline modified TiO_2 (TP).

their binding energies are 284.8, 531, 458.5, 401.3 eV, respectively. We also measured C1s and O1s core levels. The results imply that three peaks are observed at binding energies of 284.5, 286.1, and 288.2 eV for C1s and 531 eV for O1s.

The peak (284.8 eV) of C1s indicates the presence of ^1C and the peak (286.3 eV) is attributed to ^2C in the structure of PANI. The binding energy peak of N1s at 399.2 eV can be assigned to the benzenoid aniline (–NH–) structure. The binding energy (401 eV) of N1s in the nanocomposites, which is higher than that of PANI, also indicates strong interaction (e.g. hydrogen bonding) between TiO_2 and PANI (Li *et al.* 2008).

Transmission electron microscopy (TEM)

Figure 8 shows TEM images of TiO_2 and polyaniline/TiO_2 nanocomposites. The TEM image of polyaniline/TiO_2 nanocomposites shows the granular structures. The incorporation of polyaniline into the TiO_2 decreases the particle size. Bare TiO_2 shows a particle of 18 nm while the composite shows a particle size of 14 nm.

Photocatalytic activity studies

The photocatalytic activity TiO_2 and PANI/TiO_2 with different molar ratios under visible light illumination (>400 nm) was evaluated by comparing the photodegradation efficiency of 4-NP. The amount of catalyst and time was optimised by taking different amounts of catalyst and performing the reaction at different time periods. It was observed that maximum degradation efficiency was obtained at a catalyst loading of 20 g l^{-1} for a time period of 1 hour. Compared to pure TiO_2, the modified TiO_2 systems exhibit better activity under visible light irradiation.

Effect of catalyst loading

Subsequent experiments were accomplished to study the effect of the amount of TP composites on 4-NP removal efficiency at pH 6.4 and degradation time of 1 h.

The removal efficiency increases as the catalyst amount increases from 0.005 to 0.04 g, as shown in Figure 9(a). From the graph it is evident that, at first, the percentage degradation increases with the increase in amount of catalyst and beyond a certain limit the percentage degradation decreases. This may be due to a light scattering effect and reduction in light penetration through the effluent due to the obstruction of a large number of solid particles. Therefore, the optimal amount of catalyst was selected as 20 g l^{-1}.

Effect of time

To show the influence of time upon the degradation of 4-NP, the reaction was carried out over a time period of 1 hour. It is

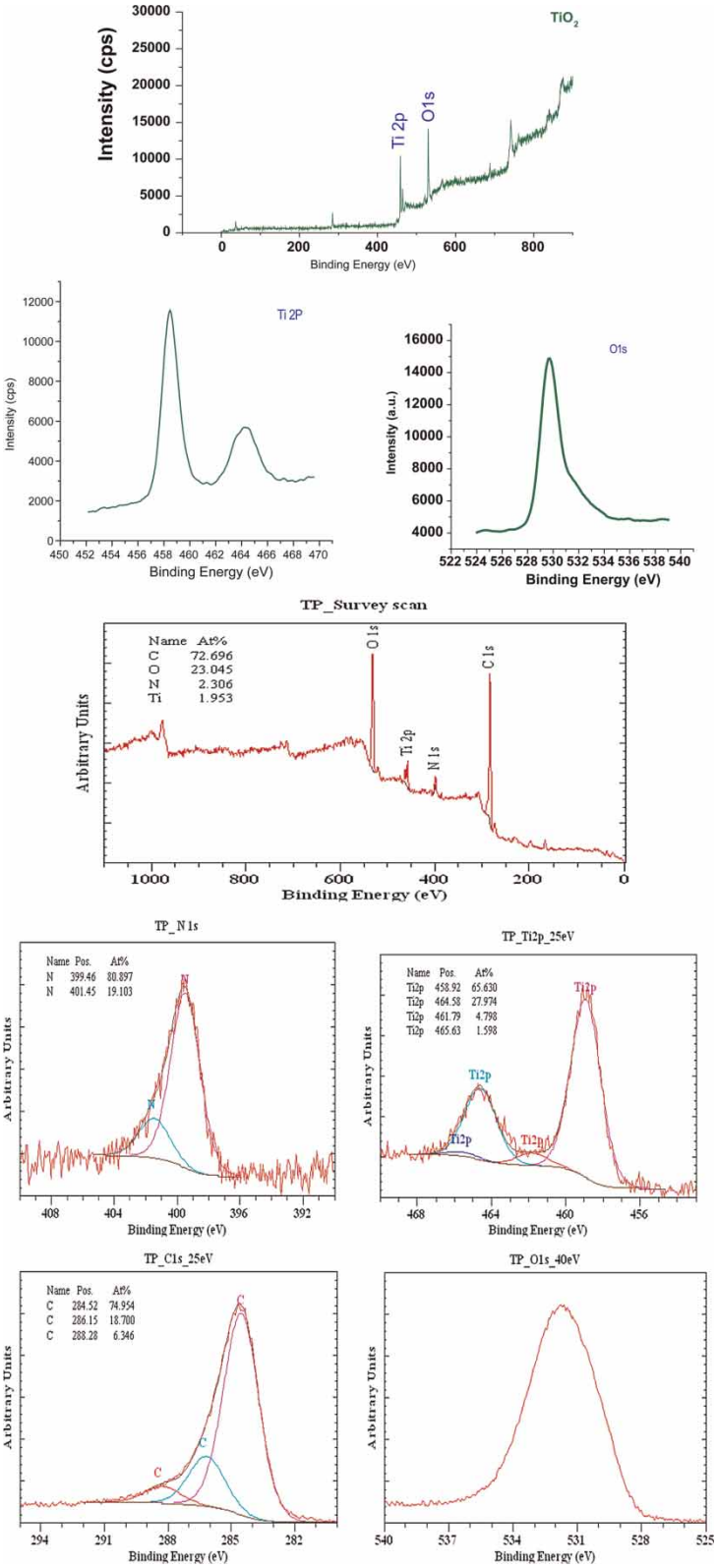

Figure 7 | XPS spectra (survey scan and core level spectra) of TiO_2 and polyaniline modified TiO_2 samples.

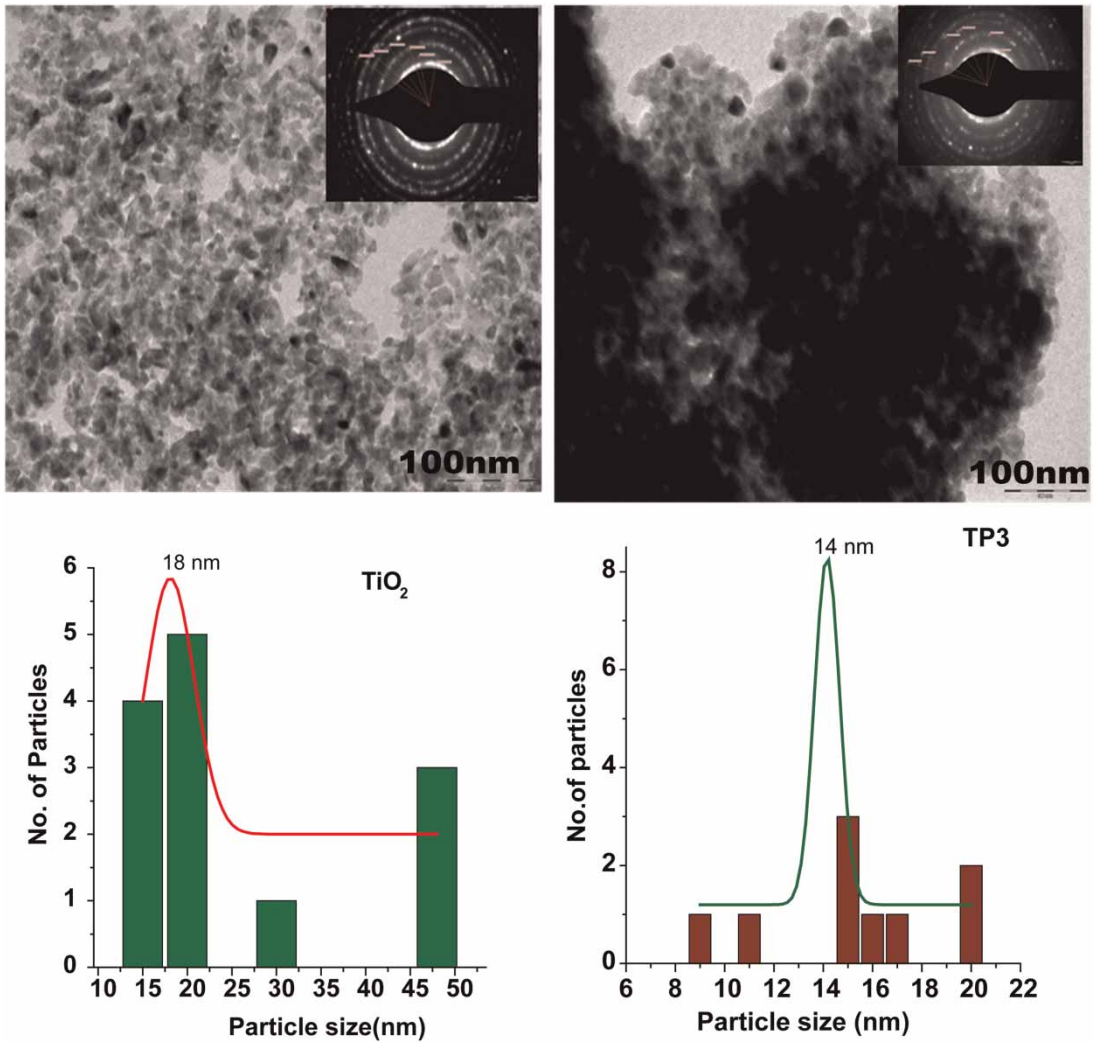

Figure 8 | TEM images and particle size histogram of TiO_2 and polyaniline modified TiO_2 samples.

seen from Figure 9(b) that as time increases the degradation increases and maximum degradation efficiency was obtained at 60 min. The initial degradation rate is higher and that may be due to more contact between the photocatalyst surface and *p*-nitrophenol. Later on the degradation rate is slower this may be due to the availability of less surface active sites on the photocatalyst surface.

Effect of pH

The degree of photocatalytic degradation of 4-NP was found to be affected by a change in pH. In order to study the effect of pH on photocatalytic degradation of 4-NP, a pH range from 2–10 was selected. Figure 9(c) shows the effect of varying the pH, from 2 to 10, on the degradation of 4-NP in the presence of TiO_2 polyaniline under visible light irradiation.

Increasing the pH of the 4-NP solution from 2 to 6, increases the degradation from 10 to 83% at 60 min. Degradation of 4-NP was high between pH 2 and 6, while the degradation efficiency was lower in the alkaline environment above pH 7. Also there is a red shift in λ_{max} as we move from acidic to alkaline pH. This is represented in Figure 9(d). Maximum degradation efficiency was obtained at pH 6. So the optimum pH for the reaction is fixed as 6 and further experiments were carried out at this pH.

Effect of polyaniline content

The polyaniline modified TiO_2 nanocomposites shows superior activity compared with the bare TiO_2. As the amount of polyaniline in the composite increases, the degradation first shows an increase and then a further increase in the polyaniline content decreases the degradation slightly. This may be because there is an optimum concentration for

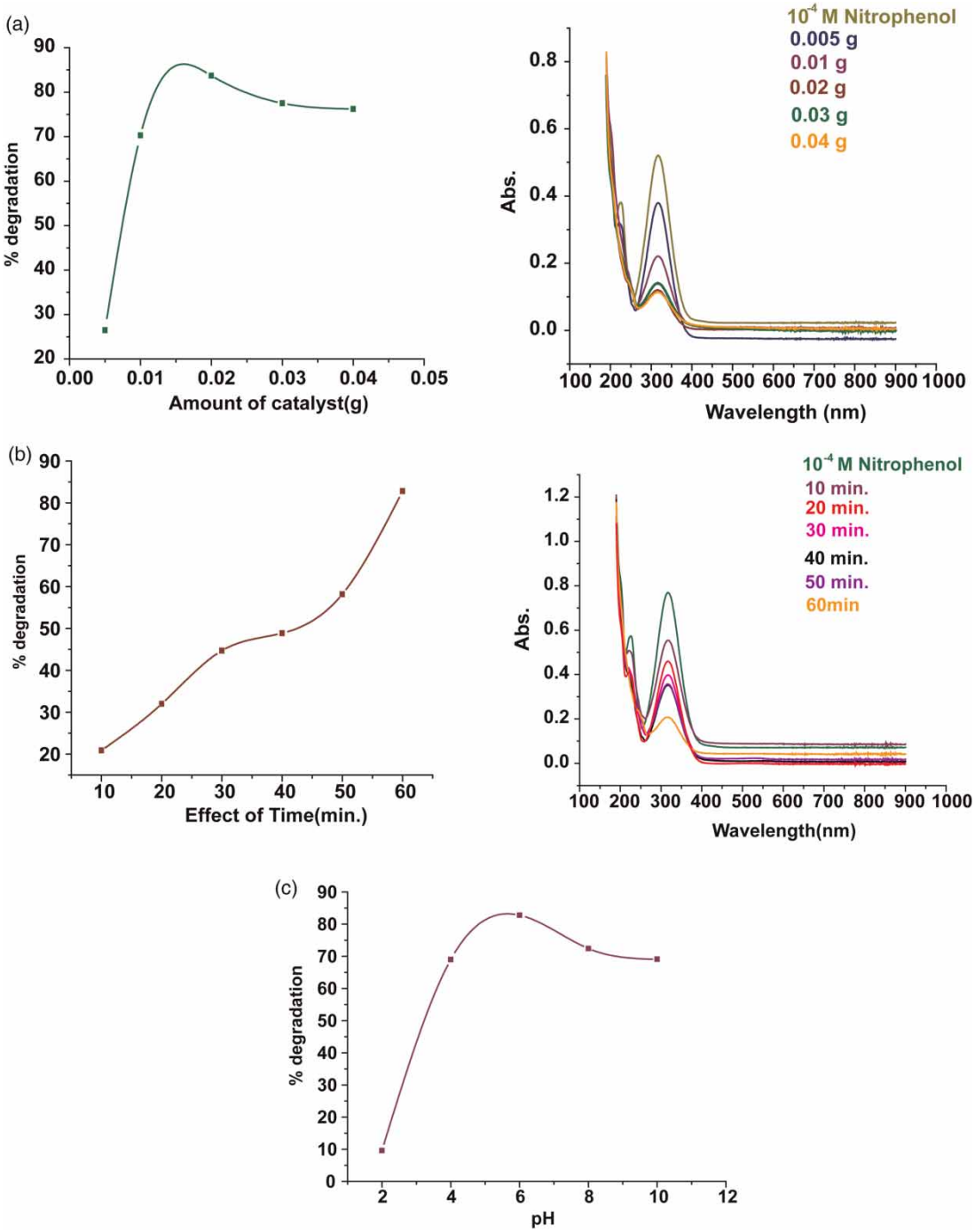

Figure 9 | (a) Effect of amount of catalyst. (b) Effect of time on photocatalytic degradation of 4-NP. (c) Effect of pH on degradation of nitrophenol. (d) Variation of absorption maxima of 4-NP in acidic and basic pH. (e) Effect of polyaniline content. (f) Recyclability study. *(continued)*

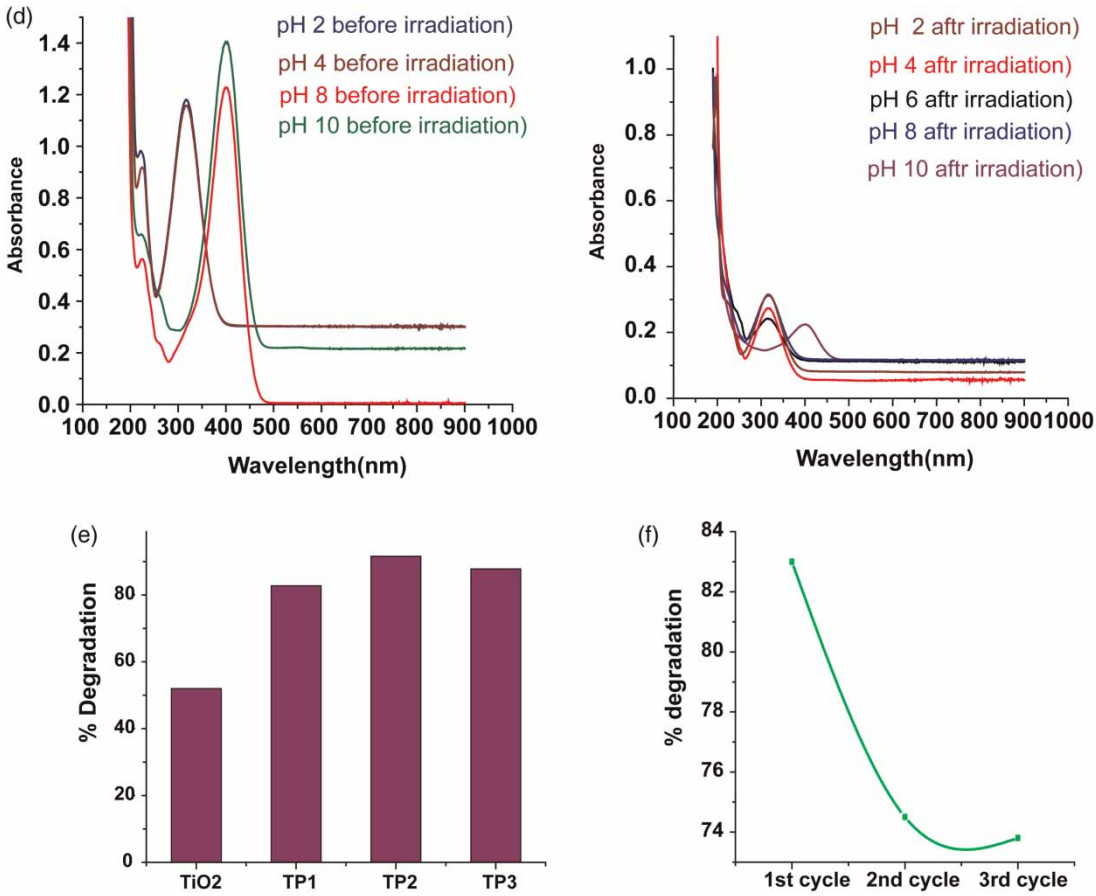

Figure 9 | continued.

high catalytic activity. Figure 9(e) shows the effect of polyaniline content on the photocatalytic degradation of 4-NP.

Recyclability

In order to check the efficiency of the catalyst the recycling study was carried out. In the first cycle, the catalyst shows a degradation of 83% and, in the second and third cycles, it decreases to about 75–73% and after that it shows a drastic decrease. Therefore, it can maintain activity only up to the third cycle. Figure 9(f) shows the recycling studies of the catalyst.

CONCLUSIONS

In this study, a polyaniline modified TiO_2 photocatalyst which was highly responsive to visible light was prepared. 4-NP is successfully degraded by TiO_2-polyaniline nanocomposite-assisted photocatalysis in an aqueous dispersion under visible light. Photocatalytic degradation of 4-NP depends on several things including the amount of catalyst, pH and polyaniline content. The prepared catalyst shows a maximum of 91% degradation within a time period of 60 min. The visible light assisted photocatalysis with TiO_2-polyaniline nanocomposites can be used as a viable technique for the treatment of 4-NP (an organic pollutant).

ACKNOWLEDGEMENTS

The authors are grateful to CSIR, New Delhi, for financial assistance and to Dr C. Anandan, Scientist, National Aerospace Laboratory Bangalore, for XPS analysis and Dr M. K. Jayaraj, Department of Physics, Cochin University of Science and Technology, for Raman analysis.

REFERENCES

Augugliaro, V., Palmisano, L. & Schiavello, M. 1991 Photocatalytic degradation of nitrophenols in aqueous titanium dioxide dispersion. *Appl. Catal.* **69**, 323–340.

Augugliaro, V., López-Muños, M. J., Palmisano, L. & Soria, J. 1993 Influence of pH on the degradation kinetics of nitrophenol isomers in a heterogeneous photocatalytic system. *Appl. Catal.* **A101**, 7–13.

Chen, D. & Ray, A. K. 1998 Photodegradation kinetics of 4-nitrophenol in TiO_2 suspension. *Water Res.* **32**, 3223–3234.

Danielle, C. S., Michelle, S. M., Ivo, A. H. & Aldo, J. G. Z. 2003 Preparation and characterization of novel hybrid materials formed from $(Ti,Sn)O_2$ nanoparticles and polyaniline. *Chem. Mater.* **15**, 4658–4665.

Ganesan, R. & Gedanken, A. 2008 Organic–inorganic hybrid materials based on polyaniline/TiO_2 nanocomposites for ascorbic acid fuel cell systems. *Nanotechnology* **19**, 435709.

Guo, Y., He, D., Xia, S., Xie, X., Gao, X. & Zhang, Q. 2012 Preparation of a novel nanocomposite of polyaniline core decorated with anatase-TiO_2 nanoparticles in ionic liquid/water microemulsion. *J. Nanomater.* Article ID 202794, http://dx.doi.org/10.1155/2012/202794 (7 pp.).

Huyen, D. N., Tung, N. T., Thien, N. D. & Thanh, L. H. 2011 Effect of TiO_2 on the gas sensing features of TiO_2/PANI nanocomposites. *Sensors* **11**, 1924–1931.

Kochany, E. L. 1991 Novel method for photocatalytic degradation of 4-nitrophenol in homogeneous aqueous solution. *Environ. Technol.* **12**, 87–92.

Krishnakumar, B. & Swaminathan, M. 2011a A convenient method for the N-formylation of amines at room temperature using TiO_2-P25 or sulfated titania. *J. Mol. Catal. A: Chem.* **334**, 98–102.

Krishnakumar, B. & Swaminathan, M. 2011b Recyclable solid acid catalyst sulfated titania for easy synthesis of quinoxaline and dipyridophenazine derivatives under microwave irradiation. *Bull. Chem. Soc. Jpn* **84**, 1261–1266.

Li, X., Wang, D., Cheng, G., Luo, Q., An, J. & Wang, Y. 2008 Preparation of polyaniline-modified TiO_2 nanoparticles and their photocatalytic activity under visible light illumination. *Appl. Catal. B: Environ.* **81**, 267–273.

Liao, G., Chen, S., Quan, X., Zhang, Y. & Zhao, H. 2011 Remarkable improvement of visible light photocatalysis with PANI modified core–shell mesoporous TiO_2 microspheres. *Appl. Catal. B: Environ.* **102**, 126–131.

Liu, J., An, T., Li, G., Bao, N., Sheng, G. & Fu, J. 2009 Preparation and characterization of highly active mesoporous TiO_2 photocatalysts by hydrothermal synthesis under weak acid conditions. *Microporous Mesoporous Mater.* **124**, 197–203.

Meallier, P., Nury, J., Pouyet, B. & Bastide, J. 1977 Photodegradation des molecules phytosanitaires II – cinetque et mecanisme de photodegradation du parathion. *Chemosphere* **6**, 815–820.

Nakagawa, M. & Crosby, D. G. 1974 Photodecomposition of nitrofen. *J. Agric. Food Chem.* **22**, 849–853.

Ohtani, B., Gawa, Y. O. & Nishimotto, S. 1997 Kinetic study of free-radical-scavenging action of flavonoids in homogeneous and aqueous triton X-100 micellar solutions. *J. Phys. Chem.* **101**, 3746–3753.

Paola, A. D., Augugliaro, V., Palmisano, L., Pantaleo, G. & Savinov, E. 2003 Heterogeneous photocatalytic degradation of nitrophenols. *J. Photochem. Photobiol. A: Chem.* **155**, 207–214.

Salem, M. A., Al-Ghonemiy, A. F. & Zaki, A. B. 2009 Photocatalytic degradation of allura red and quinoline yellow with polyaniline/TiO_2 nanocomposite. *Appl. Catal. B: Environ.* **91**, 59–66.

Yang, L., Luo, S., Li, Y., Xiao, Y., Kang, Q. & Cai, Q. Y. 2010 High efficient photocatalytic degradation of p-nitrophenol on a unique Cu_2O/TiO_2 p-n heterojunction network catalyst. *Environ. Sci. Technol.* **44**, 7641–7646.

Zhang, L., Liu, P. & Su, Z. 2006 Preparation of PANI–TiO_2 nanocomposites and their solid-phase photocatalytic degradation. *Polym. Degrad. Stabil.* **91**, 2213–2219.

First received 8 February 2014; accepted in revised form 19 June 2014. Available online 30 July 2014